Dataset for Cyclic Tests of Eleven Lightly Reinforced Concrete Walls

Yiqiu Lu[1] and Richard S. Henry[2]

Abstract

A series of reinforced concrete wall tests were conducted at the University of Auckland to address the lack of experimental data on flexure-dominant lightly reinforced concrete walls that are common in multi-storey buildings in regions of low or moderate seismicity. The experimental program comprised of eleven rectangular reinforced concrete walls that were subjected to pseudo-static cyclic loading. The tests were used to investigate minimum vertical reinforcement provisions for reinforced concrete walls and formed the basis for revisions to the New Zealand Concrete Structures Standard (NZS 3101) and the US Building Code Requirements for Structural Concrete (ACI 318). The recorded documentation and data collected throughout the test program has provided a high-quality dataset that is a valuable resource to researchers investigating the seismic behaviour of reinforced concrete walls. The dataset is published and publicly available on DesignSafe-CI (DOI: https://doi.org/10.17603/ds2-tshe-kd83). The methodology of the data collection is described and a road map for navigating the dataset is presented to support future use of the archived dataset.

Introduction

Ductile reinforced concrete (RC) walls are typically designed to form well-distributed flexural cracks in the plastic hinge region in order to spread yielding of the vertical reinforcement over a significant height. In contrast to this, during the 2010/2011 Canterbury earthquakes in New Zealand several lightly reinforced concrete walls in multi-storey buildings formed only a limited number of flexural cracks in the plastic hinge region as opposed to the expected well distributed crack patterns (Kam et al. 2011, Sritharan et al. 2014). In response to these observations, engineers and researchers questioned whether the current minimum vertical

[1] Dept. of Civil and Environmental Engineering, University of Auckland, Auckland, New Zealand, 1010.

[2] Dept. of Civil and Environmental Engineering, University of Auckland, Auckland, New Zealand, 1010.

reinforcement for RC walls were sufficient to generate the intended closely spaced flexural cracks at the plastic hinge region. However, at the time only a small number of flexure-dominant walls with low vertical reinforcement contents had been previously tested and it was difficult to evaluate minimum vertical reinforcement limits without reliable test data. To address the lack of experimental data on flexure-dominant lightly reinforced concrete walls, a series of large-scale RC wall tests were conducted at the University of Auckland. Key findings from these tests and subsequent analysis formed the basis for revisions to the minimum vertical reinforcement limits for RC walls in both the New Zealand Concrete Structures Standard (NZS 3101:2006 - Amendment 3) (2017) and the US Building Code Requirements for Structural Concrete (ACI 318-19) (2019).

The recorded documentation and data collected throughout the test series has provided a high-quality dataset that is now published on DesignSafe-CI (Rathje et al. 2017). The published dataset it titled "PRJ-1648 - University of Auckland Lightly Reinforced Concrete Wall Tests" and can be accessed using the following DOI: https://doi.org/10.17603/ds2-tshe-kd83 (Lu and Henry 2019). The objective of this paper is to provide a roadmap of the dataset for interested users with the test design and results having been published separately (Lu 2017, Lu et al. 2017, Lu et al. 2018). An overview of the experimental program is presented and the data collection procedures and the organization of the archived dataset is described, including test documentation, photos, videos and sensor data. Examples of the derived data for both global and local wall behaviour are plotted to illustrate the utility and reliability of the test data.

Data Significance

When compared to previous tests on RC walls, the dataset addresses the lack of experimental data on flexure-dominant lightly reinforced concrete walls that are commonly used in multi-storey buildings in regions of low or moderate seismicity. The unique features and variables of the test walls in the dataset include:

- All the test walls were designed with total vertical reinforcement ratios between 0.5-0.8% and with low shear demand to capacity ratios representing flexural dominate lightly reinforced concrete walls.

- The test program contained six test walls with evenly distributed vertical reinforcement and five walls

with a varying amount of additional vertical reinforcement concentrated at the ends of the wall, allowing for the influence of the reinforcement layout to be investigated.

- The walls with distributed vertical reinforcement were subjected to a range of loading demands, including spans of 2-6 and axial load ratios from 0 to 6.6%, allowing for direct comparisons of the relative performance as the design actions are altered.

The dataset summaries the results from eleven test walls including all sensor data (load cell, LVDT, string-pot displacement gauge, displacement transducer and strain gauge). Details are also provided including the test wall design, material properties, test setup, loading protocol, instrumentation plan, test sequences, test observations, crack patterns, and photos/videos that were taken throughout the tests. This unique dataset is a valuable resource to researchers investigating the seismic behaviour of RC walls. Specifically, the dataset could be used to justify revising minimum vertical reinforcement limits in seismic design standards, calibrating and validating numerical models of RC walls, developing performance-based design methodology for lightly reinforced concrete walls, assessing the seismic behaviour of existing lightly reinforced concrete walls, and identifying damage states that correspond to reparability limits for RC walls.

Test Overview

The overview of the test series is briefly described to provide information that allows the interested data users to determine whether the test data is useful and sufficient for their research. The experimental program comprised of a total of eleven large-scale rectangular RC walls that were subjected to pseudo-static cyclic loading. The test was conducted in two phases that included six walls in Phase I and five walls in Phase II designed in accordance with minimum vertical reinforcement requirements in NZS 3101:2006 (Amendment 2) (2006) and NZS 3101:2006 (Amendment 3) (2017), respectively. A summary of the main parameters for the eleven test walls is presented in Table 1, and drawings of the test wall details are shown in Figure 1. All the test walls had identical dimensions, consisting of 1.4 m (55.1 in) length, 2.8 m 110.2 in) height, and 150 mm (5.9 in) thickness. Grade 300E (f_y = 300 MPa, 43.5 ksi) reinforcing steel and 40 MPa (5801 psi) specified concrete were used in all the test walls. The eleven test walls were used to comprehensively

investigate the effect of shear span ratio (C1, C2, C3 and M1, M5), axial load (C1, C4, C5), anti-buckling ties (C2, C6), vertical reinforcement layout (C1, M5 and C6, M1), end zone vertical reinforcement ratio (C6, M1, M2, M3), end zone vertical reinforcement diameter (M2, M4) and number of reinforcement bars in end zone (M2, M4). Despite being designed with New Zealand concrete design standards, the test walls represent a range of lightly reinforced concrete walls designs that are used in multi-story buildings in many countries with low or moderate seismicity.

The test setup shown in Figure 2 simulated the expected seismic loading on the lower portion of the scaled RC wall that represented designs appropriate for tall buildings. The two vertical actuators were programmed to apply an axial load and a moment to the top of the wall that was calculated based on the real-time measurement of the force in the horizontal actuator to achieve a constant axial load ratio and shear-span ratio during tests. The lateral loading protocol was force controlled prior to the theoretical cracking moment at the wall base followed by drift control until failure. The installed instrumentation allowed for monitoring both global and local response of the test walls.

Phase I walls were tested from April to September 2014 and Phase II walls from November 2015 to May 2016. All of the eleven test walls exhibited flexure-controlled behaviour and the failure was all controlled by vertical reinforcement buckling and subsequent reinforcement fracture. The behaviour of the six Phase I test walls with the minimum distributed vertical reinforcement was controlled by 1-3 large flexural cracks at the wall base with no significant secondary cracking. The limited cracking greatly reduced the spread of the plasticity and resulted in limited ductility capacity. Large crack openings caused additional problems such as premature reinforcement buckling and fracture, large axial elongations and wall sliding. This wall design avoids potential non-ductile behaviour of walls with a higher cracking moment than yield moment, but only exhibit low ductility capacity and so are only suitable for walls designed for low or nominal ductility demands. The behaviour of the five Phase II test walls with additional vertical reinforcement at end region was controlled by a large number of primary and secondary cracks over the wall height. The distributed secondary cracking allowed the vertical reinforcement to yield over a significant length, resulting in larger plastic hinge rotation capacity when compared to the Phase I walls. The Phase II test wall detailing is suitable for walls designed for

high ductility demands in accordance with modern seismic design standards. Detailed observations, test results and discussion of the results are published separately by Lu et al. (2017, 2018).

Data collection and processing

Test procedure

The test process comprised of a number of specific steps and procedures that were recorded and formed the basis of documentation and data complied within the dataset. The procedures are summarised in Figure 3 along with the corresponding documentation and data generated for each wall test. The test procedure was separated into four main stages: 1) pre-test preparation, 2) pre-test inspection, 3) testing and 4) post-test processing. The test program began with a systematic design of the test including test wall, test setup, and instrumentation, which was followed by construction of the wall specimens (see Figure 1) and the blue steel test frames used for the setup (see Figure 2). The test wall was erected and prepared, followed by installation of the instrumentation and cameras.

A pre-test inspection was conducted prior to applying any lateral or vertical loads, including checking that all the sensors and cameras were working correctly, inspecting and marking any existing cracks on the wall, measuring as-built dimensions of test walls and as-built positions of sensors, and calibrating the positions of the two cameras used for digital photogrammetry. A photo of the initial condition of the test wall was taken after the pre-test inspection and the Data Acquisition (DAQ) was triggered from this point. The next step was to apply axial load via the two vertical actuators that were controlled to ramp vertical compression force simultaneously to prevent any accidental bending moment being applied to the wall. Global photos were taken after initial axial load was applied.

The lateral loading protocol applied to the test walls was developed in accordance with ACI 374.2R-13 (2013) and ACI ITG-5.1-07 (2008). The first four lateral-load cycles were force-controlled with load increments equal to 1/4, 1/2, 3/4 and 1 times of the force corresponding to the theoretical cracking moment at the wall base calculated using the average expected concrete strength. Global photos were taken at the peak of each cycle and zero drift, while inspections were conducted only if the wall cracked during the force-controlled cycles.

The following cycles were drift-controlled with three full cycles at each drift level applied to the wall. The target drift amplitudes were 0.2%, 0.25%, 0.35%, 0.5%, 0.75%, 1.0%, 1.5%, 2.0%, 2.5% and 3.5%. During drift-controlled cycles, global photos were taken both at each peak and zero drift for all cycles. Detailed inspections were conducted during the first and third cycles at each peak drift, including marking crack maps on the wall and on a crack map diagram, measuring crack widths, taking roaming photos of the wall and any observed damage. Residual crack widths were also measured during the first and third cycles after the wall was unloaded. Key observations, including first cracking, concrete spalling, reinforcement buckling, reinforcement fracture and concrete crushing were recorded throughout the test. The integrity of sensors was also checked throughout the test and any damaged or compromised sensors were recorded.

The overall procedure for each wall test was similar, but the loading protocol may differ slightly for each test. An excel spreadsheet “Loading protocol and procedure” was created for each wall that summarised loading cycle number, the corresponding target force and drift and actual achieved lateral force and drift measured during the test, as well as the inspection tasks that were conducted in each loading step during testing. The loading cycle number starts with 0 and counted in increments of 0.25 for each loading ramp or 1.0 for a full reverse cycle, resulting in a cycle number of X.25 at positive peak and X.75 at negative peak.

Wall details and test setup

Two files in the dataset “Wall details and test setup - Phase I” and “Wall details and test setup - Phase II” summarise the detailed design basis of the test wall parameters, drawings of test wall and details of the test setup.

Instrumentation

The test walls were instrumented with a dense array of approximately 80 sensors in order to monitor both the global and local response of the wall, as shown in Figure 4. The horizontal displacement at the top of the wall was measured using two string-pot displacement gauges (DW1 and DW2) and the forces and displacements applied by each actuator were monitored using internal load cells (lc_ah, lc_al and lc_ar) and LVDTs (d_ah, d_al and d_ar). On one face of the wall, threaded steel studs were embedded in the concrete during construction

approximately 30 mm from the wall edges. Displacement gauges were attached to these studs to measure the local deformations of different sections of the wall. The details of embedded studs prior to concrete pouring are shown in Figure 5. The steel studs were tied to the corner vertical reinforcement and covered by wax tape on the top to protect the thread in the stud during concrete pouring. A total of 9 displacement gauges were placed along each edge up the height of the wall to monitor axial strains and curvatures (P21-P36). Shear deformations in the wall were measured using displacement gauges positioned in an "X" configuration over two panel regions, as shown in Figure 4 (P37-P40). To accurately capture the cracking at the wall base, two rows of 5 displacement gauges were placed along the wall length that extending 300 mm up the wall height (P44-P53). Steel studs were also welded directly onto the corner vertical reinforcement to measure average reinforcement strains, as shown in Figure 5. These steel studs were surrounded by a thick layer of wax tape during concrete pouring. The tape was removed prior to the test so that the steel studs passed through recesses in the cover concrete to allow the average reinforcement strains to be measured using external displacement gauges over a 150 mm gauge length (P1-P20). A tension test was conducted on three samples of reinforcing bars with the welded studs attached. The fracture point typically occurred outside of the welded location and so the attachment of the studs was considered negligible to the reinforcing bar properties. Strain penetration of the vertical reinforcement at the wall-foundation interface was measured using a displacement gauge connected to the bottom stud welded on the vertical reinforcing bar and foundation (P61 and P62). Three concrete strain gauges were embedded in the two ends of the wall at different height to measure the concrete strain (cg1-cg6). Displacement gauges were also used to measure any potential vertical and horizontal slip at the wall-to-foundation, wall-to-loading beam, and foundation to strong-floor joints (P54-P60).

The instrumentation was installed as designed and the as-built dimensions were measured prior to testing. The instrumentation for each wall was summarised in a single spreadsheet that contains an instrumentation summary, as-designed dimensions and as-built measured dimensions. The "Instrumentation summary" sheet contains a drawing of the instrumentation layout and a table summarising each sensor's name, calibration factor, sensor function and positive direction. The as-designed dimensions of each sensor are marked in the instrumentation drawing in the "Designed dimension" sheet and the as-built dimensions of the sensors are listed in the "As-built dimension" sheet. During measuring as-built instrumentation dimensions, the wall was

assumed sitting in a plan coordinate with origin point at the intersection of the east edge of the wall and wall base. X and Y coordinate were defined as the directions of wall length and wall height, respectively. The measured coordinate locations for each point were recorded and the as-built dimensions of the instrumentation were determined accordingly. It should be noted that the overall instrumentation designs for all the tested walls are similar but the actual instrumentation position and/or name vary slightly for each wall. As such, the user should refer to the instrumentation spreadsheet of the particular wall being investigated.

Material testing

Grade 300E reinforcing steel produced by Pacific Steel Group in accordance with AS/NZS 4671 (2001) was used in all of the test walls. Samples of the reinforcing bars were tested from the same batch of bars used to construct each of the test wall phases. In Phase I test, three samples of each type of reinforcing bar were tested to confirm their stress-strain behaviour whereas for Phase II test, six samples were tested. The calculated stress and strain data are archived in separate spreadsheets for each reinforcing bar type for each test phase. The stress was determined by the recorded force divided by the nominal area of the reinforcing bar and the average strain was determined as the uniform elongation over a 100 mm gauge length. The test setup for the reinforcing bar testing and an example of the stress-strain relationship for the D10 bars used in Phase I test are shown in Figure 6. Key parameters such as yield strength, ultimate strength and average ultimate strain were summarized in Lu (2017) which is also archived in the dataset as a report. For reinforcing bars with no obvious yield plateau, the yield strength was taken as 0.2% proof force divided by the nominal area of the bar. The ultimate strain ε_u was chosen as the strain at maximum stress.

Six concrete cylinders with a diameter of 100 mm and a height of 200 mm were constructed alongside each wall panel with three cylinders used for compression tests and the other three used for split cylinder tests to estimate the tensile strength (f_t). All of the concrete cylinders were cured in ambient conditions beside the test walls and tested at the same day of the wall. Detailed stress and strain data were recorded during compression tests with the stress determined from the recorded force divided by the measured area of the cylinder and the strain determined from the average displacement of two LVDTs with a gauge length of 100 mm. The recorded tensile strengths were the average splitting tensile strengths calculated directly from the test conducted in

accordance with NZS 3112.2 (1986). The stress-strain compression data and the tensile strength data were archived in separate spreadsheets for each wall in the dataset. The setup for concrete cylinder testing and an example of the compression stress-strain relationship for concrete used for Wall C1 is shown in Figure 7. The key test results including compressive strength, modulus of elasticity and tensile strength are summarized in Lu (2017). The modulus of elasticity (E_c) was determined as the secant stiffness from the origin to 50% of the peak concrete compressive strength.

Media

Three digital SLR cameras and two GoPro cameras were used to record the overall and local behaviour of the wall during testing. Figure 8 shows the camera plan as well as an example of the views of each camera. A Cannon camera was set at north of the test wall to take global view photos of the whole wall and setup. Two Nikon cameras were set to the south of the test wall. The view of these two cameras focused on the wall base and included 2/3 of the wall height, as shown in Figure 8. One camera was square on to the wall and the other was located aside with a view angle of 15-20 degree. While monitoring the crack pattern and failure modes of lower part of the wall, these two cameras were also used to try a digital image correlation system with a combination of a random pattern of black dots that were painted on the southern face of the wall. These three global cameras were remotely controlled by digiCamControl software to synchronise camera capture times and name the photo files when transferred. The two GoPro cameras were installed to capture corner views at wall base on each side of the wall. It should be noted that the positions of the cameras were not measured precisely for each test. The still camera plan for all the tested walls was similar but the camera views are slightly different for each wall due to these exact positions and zooms. In addition, a roaming camera was used to take inspection photos in accordance with a photo checklist covering both global and local condition of the wall.

Prior to testing, a series of calibration photos were taken of a calibration checkerboard at different locations to determine the position of the two cameras used for photogrammetry. Global photos for the northern and southern cameras were taken prior to testing, after applying axial load, at peak and zero drift points during all cycles and at zero force unloading from peak during all cycles. The corner photos for the two GoPro cameras

and roaming photos were taken only at peak drifts during the first and third drift-control cycles when inspections were performed. Photos of the final condition of the test wall with and without sensors were also taken at the conclusion of the test. While the test was monitored mostly by still images, videos were also recorded during some tests by the roaming camera. In addition, the photos from the northern camera were used to edit time-lapse videos for walls C1, C2, C6 and M1 to illustrate the overall crack and damage progression. All of the photos, videos and time-lapse animations were collected and archived in the dataset.

Crack pattern and width

Crack maps were drawn and crack widths were measured at peak drifts during the first and third drift-control cycles to each drift level. Crack maps were recorded on a white paper and were drawn based on a photo-copy of the crack map drawn at the previous step. An example of the drawn crack maps and measured crack widths for wall M4 during the first cycle at ±1.0% lateral drift is shown in Figure 9. The crack patterns visible on both the north and south sides of the wall were similar, and so the crack pattern figures were drawn only from the southern side. It should be noted that in the crack pattern drawings, the left side is west and right side is east, as shown in Figure 9. Cracks during load steps in the direction of drift to the west (or positive drifts) were marked as red and cracks in the opposite direction (negative drifts) were marked as blue. However, for the first test wall C1, the cracks were all marked as black colour regardless of the load direction. The measured crack widths at peak drifts were recorded beside the crack on the paper crack maps. The residual crack widths were also measured when the wall was unloaded to zero force for Phase I tests or when the wall was in zero drift for Phase II tests. The residual crack widths were recorded beside the peak crack width in the paper crack maps. There was one crack map with peak and residual crack widths for each inspection step, as shown in Figure 3. All these crack maps were scanned and combined into a single PDF file for each test wall.

Observation notes

Key observations, including first cracking, concrete spalling, reinforcement buckling, reinforcement fracture and concrete crushing were recorded throughout the test. Several displacement gauges at the wall base were compromised after reinforcement buckling or concrete crushing in the later stage of the testing. These

observations were recorded and the data from these sensors is unreliable after the sensors were compromised. The observational notes were digitalized into two excel spreadsheets that recorded key damage progress and sensor availability during testing, respectively.

Sensor data processing

The DAQ system was triggered prior to applying any vertical or horizontal loads to the wall. The data was recorded at a frequency of 5 HZ for all the wall tests. The raw data comprised of several TXT files due to the pausing of the test and/or restarting the DAQ system. The raw measured data can be expressed as Eq. (1), where R is the recorded data, A is the absolute voltage of the sensor, T is the initial voltage of the sensor (tare data), and C is the calibration factor.

$$R = (A - T) \cdot C \tag{1}$$

The calibration factor C was input in the DAQ system and so the raw data values are in the units of measurement rather than voltages. The unit for channels of LVDTs, displacement transducers and string-pot displacement gauges was mm and kN for load cells. All the sensors were tared when the DAQ system was triggered. Therefore, the data of all the sensors start from 0 and the measured data (R) is the relative change of the sensor readings rather than absolute value of the sensor readings. When the DAQ system was paused and restarted, the DAQ was not tared and instead an offset was applied equal to the initial tare voltage T recorded in the first raw data file.

The raw data was output in separate files and the channel names were numbered automatically by the DAQ system rather than the actual instrumentation name. Therefore, the raw data was processed in accordance with the following steps (also shown in Figure 10):

1. Combine the separate data files into a single file in chronological order.
    a. Delete the file headings and combine the separate files together into one single file.
    b. For the “time” channel, the time data commenced from 0 in each separate file whereas the time data was modified to be continuous in the combined file. For all other channels, the data

was combined without any modification.

c. Each channel was assigned a name corresponding to the instrumentation name for each wall, as summarised in the "Instrumentation summary" spreadsheet.

2. The raw data was filtered in a range of 0.5 HZ to 0.0000001 HZ using both low and high pass filters. Figure 10 shows an example of the filtering applied to channel DW1 for wall C1.

The processed data was saved into both Matlab DAT file and TXT file formats. The lateral hysteretic response is critical data that is expected to be frequently used for investigating the global response and calibrating numerical or analytical models. As such, the moment-displacement data was calculated from the processed data and saved in a single excel spreadsheet for each wall for the convenience of data users. The sensor availability spreadsheet should be referred to when using the data to check the reliability of sensor data at specific stages of each test.

Data organization

The dataset is archived in DesignSafe-CI (https://www.designsafe-ci.org/) and the structure of the dataset is shown in Figure 11. Using the DesignSafe data depot system, a dataset is archived in specific experiments that are created under an overall project. In each experiment, the system defines five categories, consisting of: 1) *Model Configuration* for information regarding the overall test design; 2) *Sensor Information* for instrumentation plans; 3) *Event* for files generated during unique test event; 4) *Report* for overall information about the entire project or experiment; 5) *Analysis* for additional analysis of the test results. The documentation and data files in the dataset can be assigned to the corresponding category to create a data structure or tree. It should be noted that Sensor Information is a sub category of Model Configuration and Event is a sub category of Sensor Information. The structure of these five categories in DesignSafe-CI is shown in Figure 11-d.

The dataset presented herein is archived in the project PRJ-1648 University of Auckland Lightly Reinforced Concrete Wall Tests with a total size of approximately 155 GB. Two Experiments "Phase I – Current design practice" and "Phase II – Modified designs" were listed within the project. In both experiments, a read me file

and a report are attached in the Report category to provide an overview of the project and the test program. The files associated with the six C walls (Wall C1, Wall C2, Wall C3, Wall C4, Wall C5 and Wall C6) are archived in Experiment "Phase I – Current design practice" and the files associated with the five M walls (Wall M1, Wall M2, Wall M3, Wall M4 and Wall M5) are archived in Experiment "Phase II – Modified designs". The data organization for all the test walls was identical and an example of wall C1 is shown in Figure 11-b. The Wall Configuration is named after the test and in each Wall Configuration, a Sensor Information named after the test "Wall C1 - Instrumentation" is attached and an Event named after the test "Wall C1 – Test data" is attached under the Sensor Information. In the Model Configuration category, there are two files and two folders "C1 – Concrete cylinder test", "Wall details and test setup – phase I", folder named "Loading protocol" and folder named "Phase I – Reinforcement test". In the Sensor Information category, a folder named "Instrumentation" is included. In the Event category, four folders named "Test observation", "Crack maps", "Media" and "Sensor data" are included. The content of each file or folder is briefly explained in the following sections.

Read me file: The read me file summaries the organization of the dataset and the types of data available.

Report: The test objectives, test programs and test results are described in Chapter 2 and Chapter 5 of the thesis tagged as a report.

Wall details and test setup: The details of the wall specimen and test setup are described in the PDF file "Wall details and test setup – phase I (Phase name)".

Concrete cylinder test: The results and raw data from concrete tests for each wall are provided in the excel file named after the test, e.g. "C1– Concrete cylinder test".

Reinforcement test: The results and raw data from tension tests of each reinforcement sample are summarized in a single excel spreadsheet in the folder named after the phase, e.g. "Phase I – Reinforcement test". The spreadsheet named as "P1 (Phase name) _ D10 (Reinforcement type) _ 1 (Sample No.)".

Loading protocol: The loading protocol spreadsheet is named after the test, e.g. "C1– loading protocol and test sequences".

Instrumentation: The instrumentation spreadsheet is named after the test, e.g. “C1 - Instrumentation” that contains instrumentation summary, as-designed dimensions, and as-built dimensions.

Crack maps: PDF files named after the test, e.g. “C1 – Crack maps” provides the scanned crack maps and measured crack widths at different loading steps.

Media: The media folder has three sub-folders named “testing photos”, “testing time-lapse” and “testing videos”, as shown Figure 11-c. The testing photo folder contains four sub-folders, including “Global photos at north”, “Global photos at south”, “Roaming photos”, “Photos at final condition”, “Calibration photos” and “GoPro photos”. The filenames of the photos in the folders of “Global photos at north” and “Global photos at south” correspond to the loading step. For example, “Canon_1837_Cycle-6.75.JPG” in the folder of “Global photos at north”, “Cannon_1837” is the camera name and the photo series number, while “Cycle-6.75” refers to the actual loading step that the photo was taken. The loading steps are summarised in the spreadsheet called “loading protocol and test sequences” in the loading protocol folder. In the folder named “Global photos at south”, the photos are separated into two folders, “camera 1” and “camera 2”. In the roaming photo folder, the photos were stored in chronological order. Before inspection photos were taken, a photo of the white board that recorded the loading step and drift ratio was taken. Therefore, the inspection photos after this photo correspond the loading step that shows in the white board, as shown in Figure 12. The folder of “GoPro photos” is separated into “GoPro 1” and “GoPro 2”. Photos of damage states of the wall taken at the end of the test are stored in the folder of “Photos at final condition”. Videos and time-lapse videos are stored in the folders of “Testing videos” and “Time-lapse videos”, respectively.

Sensor data: This folder contains a “Processed data” folder, a “Raw data” folder and the sensor availability spreadsheet named after the test, e.g. “C1 – Sensor availability summary”. The processed data is available in two formats (DAT and TXT) named after each test wall, e.g. “C1_Test data” and the moment-displacement spreadsheet named after the test, e.g. “C1 – Hysteric curve” is archived in the “Processed data” folder.

Test observation: An excel spreadsheet named after the test, e.g. “C1 - Test observation” that summarises the key observations for each test.

Derived Data

This section provides several examples of experimental results that can be plotted using the data to illustrate how to use the data and to demonstrate the reliability of the data. More extensive test results and data analysis can be found in Lu et al. (2017, 2018).

Global response

The test results highlighted that the additional end region vertical reinforcement could improve the secondary cracking behaviour of lightly reinforced concrete walls. Using the data from the crack maps and crack widths available in the published dataset, the cracking response of each of the test walls could be evaluated and compared. Figure 13 includes the measured crack widths up the wall height observed during the first cycle to 2.5% lateral drift for the test walls C6, M1 and M2. These three walls were nominally identical expect that wall C6 had a distributed reinforcement ratio while wall M1 and M2 had an end region reinforcement ratio of 1.0% and 1.4%, respectively. As shown in Figure 13, the number of cracks observed and recorded for wall M1 and M2 were significantly greater than that of wall C6 and as a result the crack spacing was reduced. Furthermore, the maximum crack widths at 2.5% drift for wall M1 and M2 were around 7 mm and 5 mm, respectively, significantly smaller than the 20 mm wide cracks that were measured for wall C6. This confirmed that concentrating additional vertical reinforcement in the ends of the wall could significantly improve the cracking behaviour of lightly reinforced concrete walls that might otherwise be controlled by discrete widely spaced cracks.

As described in the test overview section, a combination of moment, shear, and axial loads were applied to the top of the test wall to simulate seismic loading of taller RC walls using a series of three actuators. Second order effects due to the applied lateral displacements were considered in the actuator control programming to determine the forces of the two vertical actuators. The bending moment acting at the wall base can be derived from these three actuator readings with and without considering second order effects. By using the method without considering second order effects, the bending moment at wall base is simply calculated by the force of actuators multiplied by the distance that the actuators are located from the centroid of wall base. However,

for the method considering second order effects, the angles of the three actuators and their force component needs to be derived using the measured displacements from the actuator internal LVDTs and the bending moment at wall base can be calculated using the derived angles and force components. The detailed derivation methods are explained in the read me file included in the Report category of the dataset. Figure 14 compares the moment-displacement response calculated for an example of wall M2 with and without considering second order effects. The hysteric curves differ slightly using these two methods with a difference ranging between 0 to 3%. The moment-displacement response of all the 11 test walls were derived considering the second order effects and were saved in the "Processed data" folder of the dataset. The global hysteric response for all the test walls were compared with the calculated results using numerical models generated in VecTor2 (Lu and Henry 2017). The model captured the measured response of the test walls accurately, further confirming the reliability of the measured sensor data.

Local behavior

To investigate the sources and mechanisms of deformation of the wall panel, the wall was split into four flexural deformation components F1, F2, F3 and F4, as shown in Figure 15, as well as the shear deformation component. The deformation components were derived from the data of vertical displacement gauges along both wall edges (P21-P36) and the shear diagonal displacement gauges (P37-P40). The detailed calculation methodology was described by Lu et al. (2017). An example of the contributions of the five displacement components during the first cycle to each lateral drift target is shown for wall C1. The summation of these five displacement components correlated well with the wall overall lateral displacement measured directly using string-pot displacement gauges, with a difference typically less than 10%, indicating the data from these displacement gauges (P21-P40) are reliable. In addition, the flexural displacements were considerably larger than the shear displacements which was expected due to the small designed shear demand to capacity ratio. Furthermore, the measured response and the observed crack pattern collated well. The flexural deformations in the bottom portion of the wall panel contributed the majority of the wall lateral deformation, confirming the wall behaviour was dominated by 1-2 main flexural cracks at the wall base.

The average tensile strains measured along the extreme vertical reinforcement up the height of the wall can be

plotted by using the displacement gauges P1-P20. An example of the strain profile of the vertical reinforcement for wall C1 is shown in Figure 16. The strains were obtained by dividing the readings from the displacement gauges welded onto the vertical reinforcement (see Figure 4) by the as-built gauge length recorded in the "As-built dimension" in the spreadsheet "Wall C1 - Instrumentation". The reinforcement strains in the test walls were inconsistent up the wall height, with inelastic strains concentrated at crack locations, further confirming the concentrated inelastic deformations at one or two flexural cracks. It should be noted that the spreadsheet "C1 – Sensor availability summary" should be used to check whether any displacement gauges were compromised during testing. "C1 - Sensor availability summary" indicates that the displacement gauges P1 and P2 were compromised after the reinforcement buckled during the second cycles at 1.5% lateral drift. Therefore, the bottom two strains measurements should not be plotted at lateral drifts of 2.0% and 2.5%, as shown in Figure 16.

Summary

A series of experimental tests of large-scale RC walls were conducted to address the lack of experimental data on flexure-dominant lightly reinforced concrete walls. The experimental program comprised of a total of eleven large-scale rectangular RC walls that were subjected to pseudo-static cyclic loading. The test walls could represent an extensive range of lightly reinforced concrete walls that are used in multi-story buildings in many countries with low or moderate seismicity. The test walls were instrumented with a dense array of sensors and cameras that allowed for monitoring both global and local response of the walls. The documentation and data recorded throughout the test, including details of the test walls, material properties, test setup, instrumentation plan, loading protocol, test sequences, test observations, crack patterns, photos, videos, time-lapse animations, and sensor data, has provided a high-quality dataset that can be used to further improve understanding of the seismic behaviour of lightly reinforced concrete walls.

The dataset is published in the project PRJ-1648 in DesignSafe-CI and is available being viewed and downloaded for future use. The documentation collection methodologies, data processing details and the organization of the dataset was described to provide a roadmap of the dataset for interested users. Several examples were also plotted to illustrate the usefulness of the data and demonstrate the reliability of the data.

The dataset from this comprehensive test program will support a variety of future investigations, including but not limiting to justify revising minimum vertical reinforcement limits in seismic design standards, calibrating and validating numerical models of RC walls, developing performance-based design methodology for lightly reinforced concrete walls, assessing the seismic behaviour of existing lightly reinforced concrete walls, and identifying damage states and the corresponding reparability limits for RC walls.

Data Availability Statement

Some or all data, models, or code generated or used during the study are available in a repository or online in accordance with funder data retention policies. The data can be accessed as PRJ-1648 on DesignSafe-CI (https://www.designsafe-ci.org/) or directly linked from the doi below. Dataset citation:

Lu, Y. and Henry, R. S. (2019). University of Auckland Lightly Reinforced Concrete Wall Tests, DesignSafe-CI. https://doi.org/10.17603/ds2-tshe-kd83.

Acknowledgements

The authors would like to acknowledge the funding provided by the Natural Hazards Research Platform, China Scholarship Council (CSC), and the Building Performance Branch of the New Zealand Ministry of Business, Innovation and Employment (MBIE), in addition to project support and management provided by the UC Quake Center. The authors also appreciate the testing supplies that were donated by Wilco Precast, Sika (NZ) Ltd., and Fletcher Reinforcing and the assistance of R. Gultom, J. O'Hagan, D. Ripley, J. Quenneville, M. Byrami, R. Reichardt, K. Twigden, A. Jones, I. Miroslav, P. Seifi, A. Shegay, D. Duchet, A. Michard, T. Zhang, J. Naidoo, S. Smith, A. Virtue, and A. Ciputra. Finally, the support of K. Strmiska and M. Esteva during the data publication on DesignSafe-CI is greatly appreciated.

Tables

Table 1 Details of all eleven test walls

Phase	Wall	Shear span ratio	Axial load ratio	Shear demand to capacity ratio	Vertical reinforcement ratio (%)			End zone Reinforcement	End zone length (mm)	Horizontal reinforcement ratio (%)	End ties (mm)	Web ties (mm)
					End zone	Web region	Total					
I	C1	2	3.5%	0.42	Evenly distributed		0.53	N/A	N/A	0.25	N/A	N/A
	C2	4	3.5%	0.21			0.53			0.25		
	C3	6	3.5%	0.14			0.53			0.25		
	C4	2	0	0.26			0.53			0.25		
	C5	2	6.6%	0.53			0.53			0.25	R6@90	
	C6	4	3.5%	0.23			0.53			0.25	R6@60	
II	M1	4	3.5%	0.26	1.00	0.47	0.67	4 D10	210	0.25	R6@60	R6@150
	M2	4	3.5%	0.29	1.44	0.47	0.80	4 D12	210	0.25	R6@60	R6@150
	M3	4	3.5%	0.25	0.72 (1.0)	0.47	0.58	2 D12	210 (150)	0.25	R6@60	R6@150
	M4	4	3.5%	0.29	1.28	0.47	0.75	2 D16	210	0.25	R6@60	R6@150
	M5	2	3.5%	0.52	1.00	0.47	0.67	4 D10	210	0.25	R6@60	R6@150

Figures

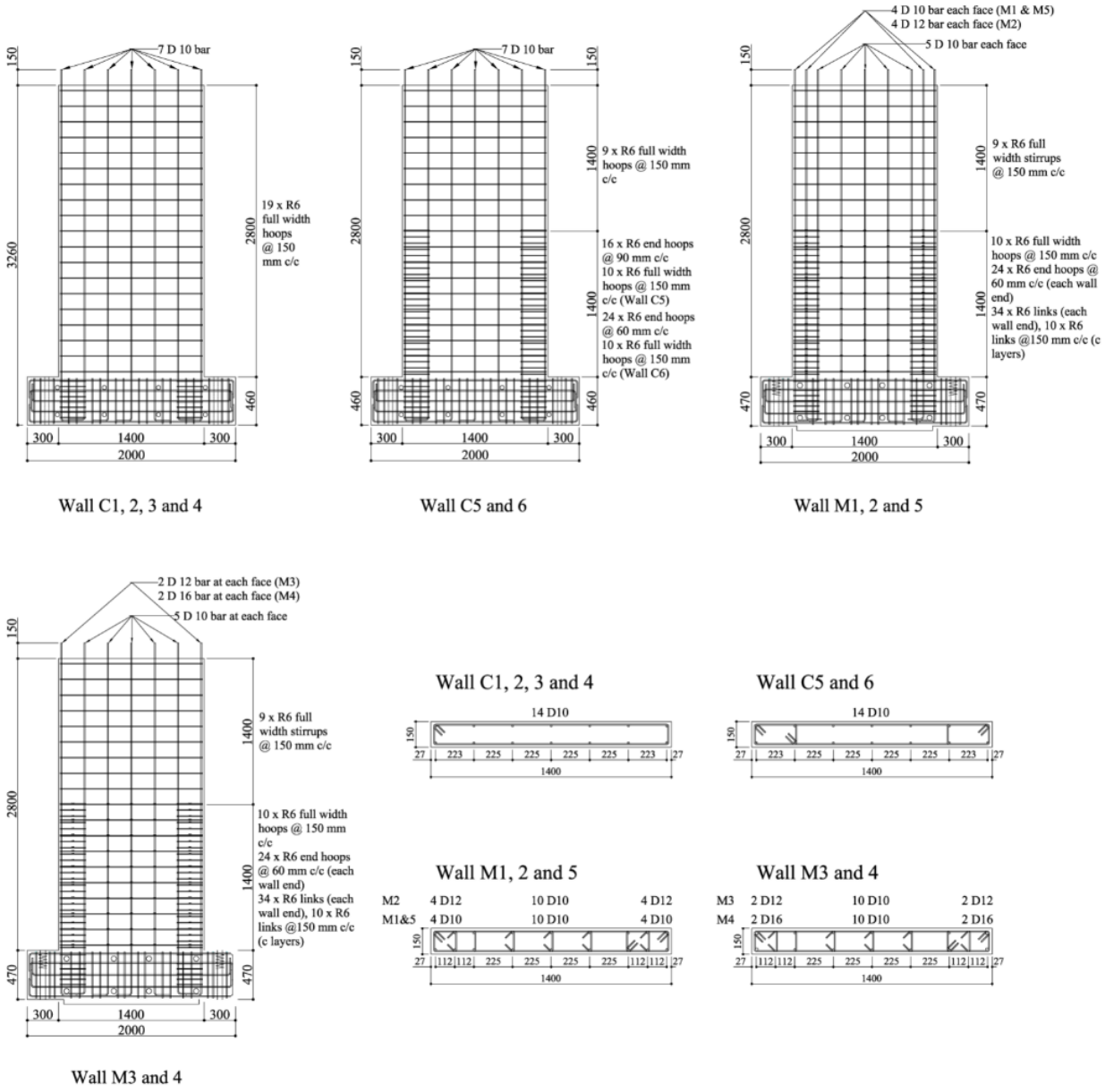

Figure 1 Details of test wall specimens

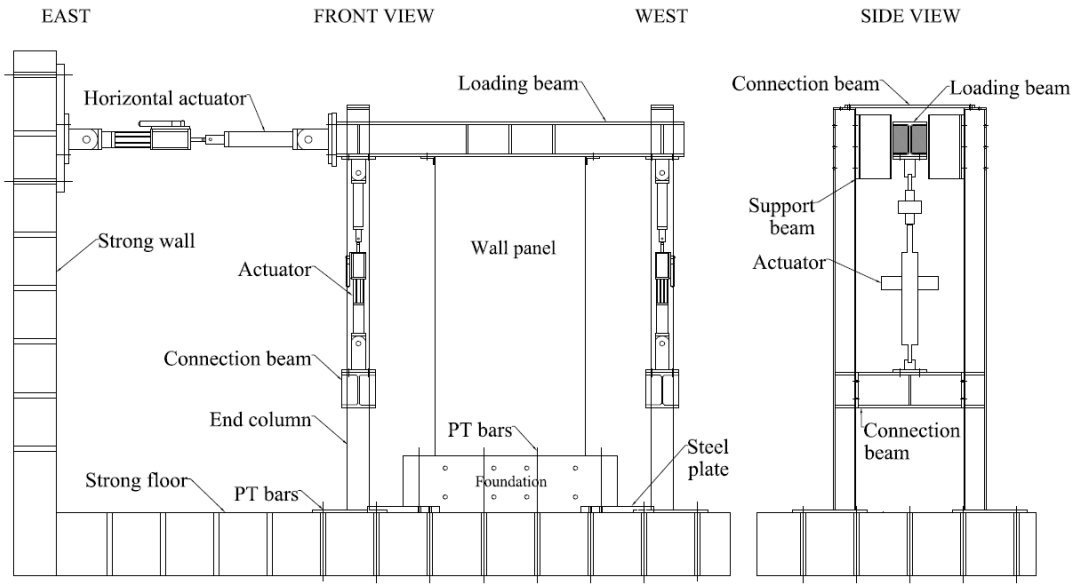

(a)

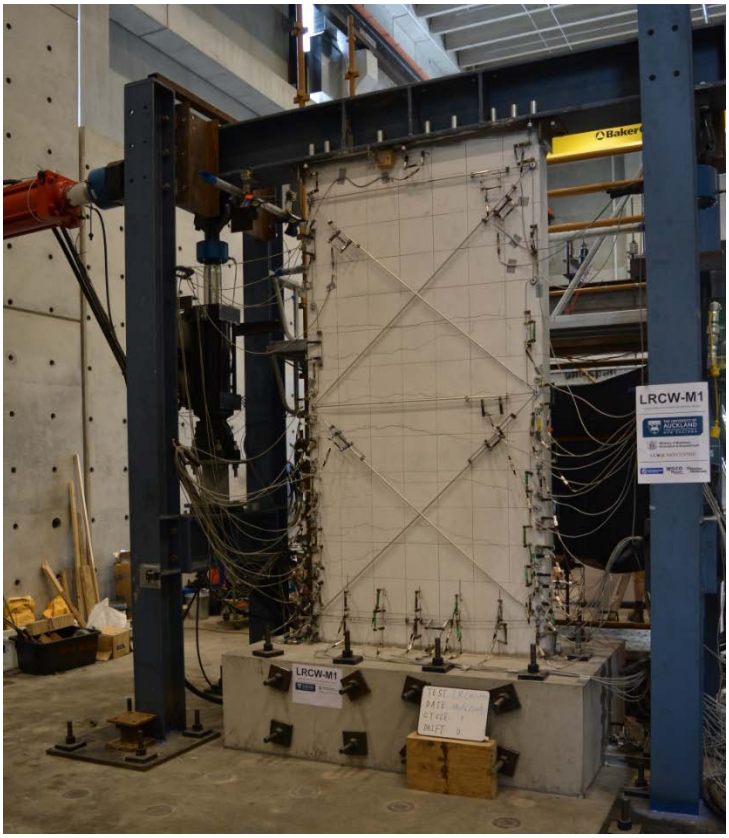

(b)

Figure 2 Test setup: (a) test setup illustration; (b) photo of test setup in lab

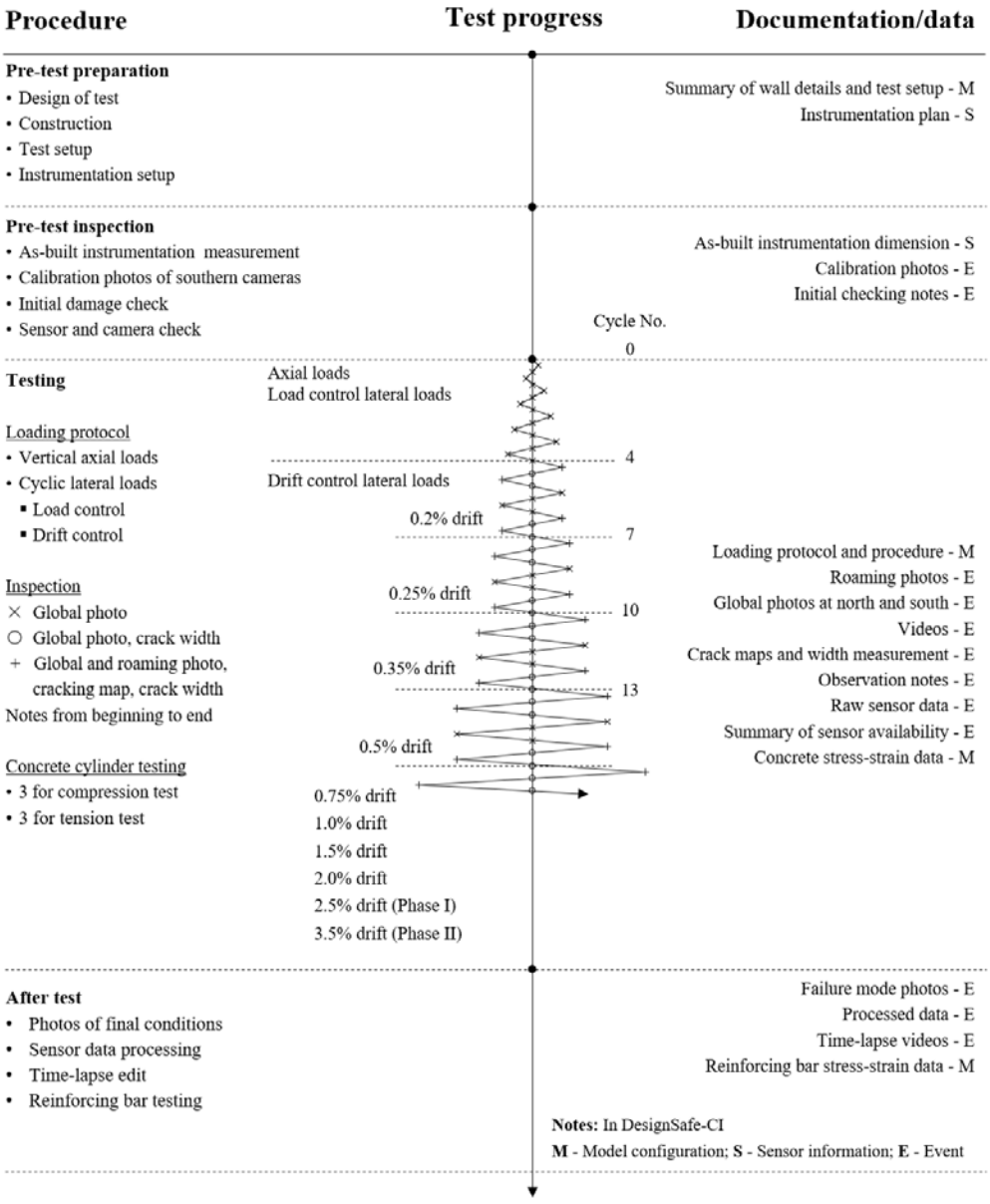

Figure 3 Test procedure and data collection

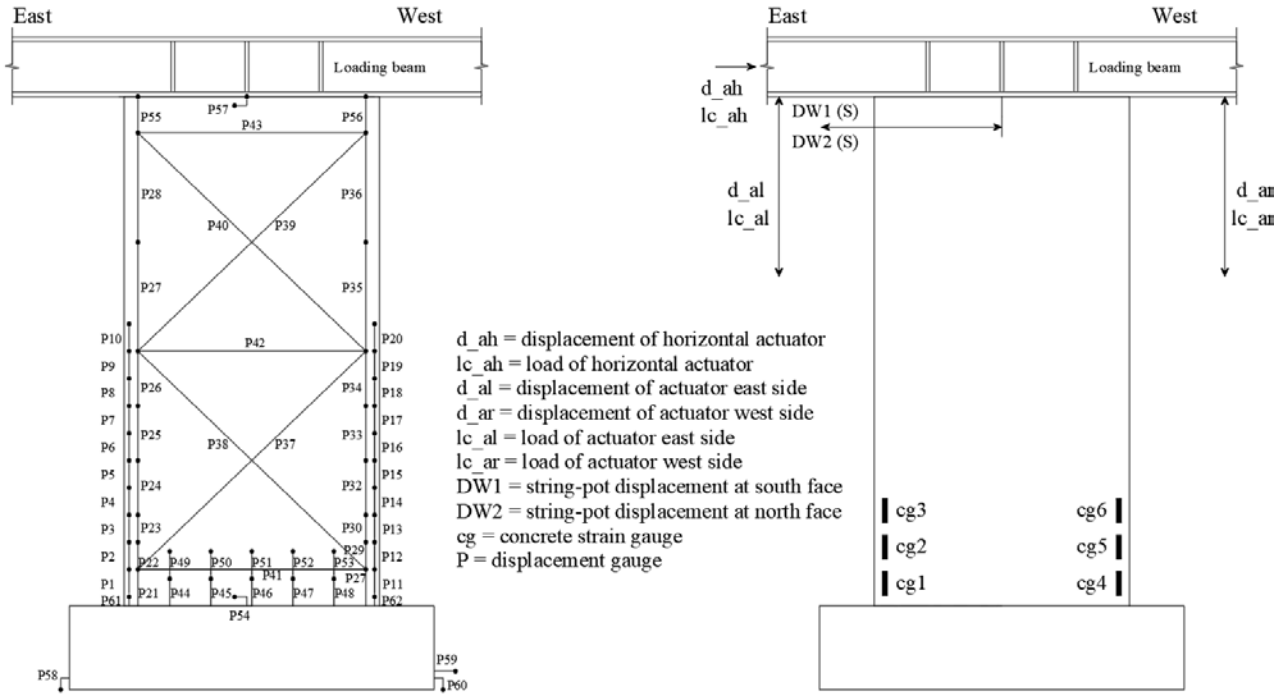

Figure 4 Instrumentation used for the test walls

(a) (b) (c)

Figure 5 Details of steel studs: (a) steel studs; (b) stud protection; (c) steel studs during test

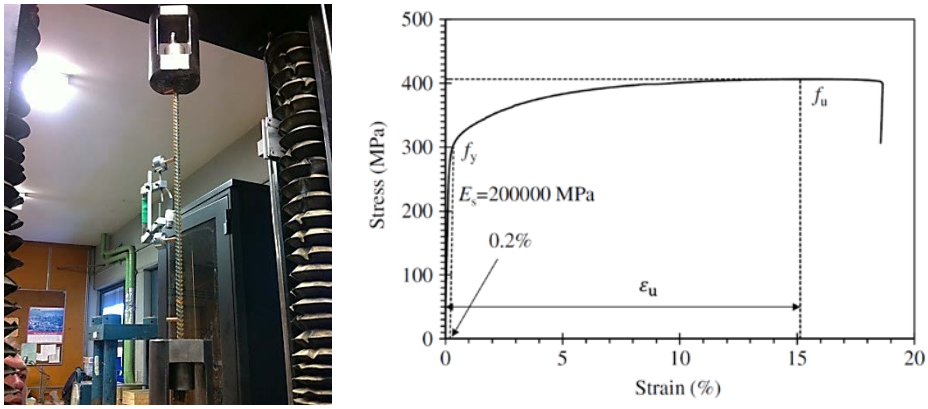

(a) (b)

Figure 6 Reinforcing bar test: (a) test setup; (b) stress-strain for D10 reinforcement in Phase I test

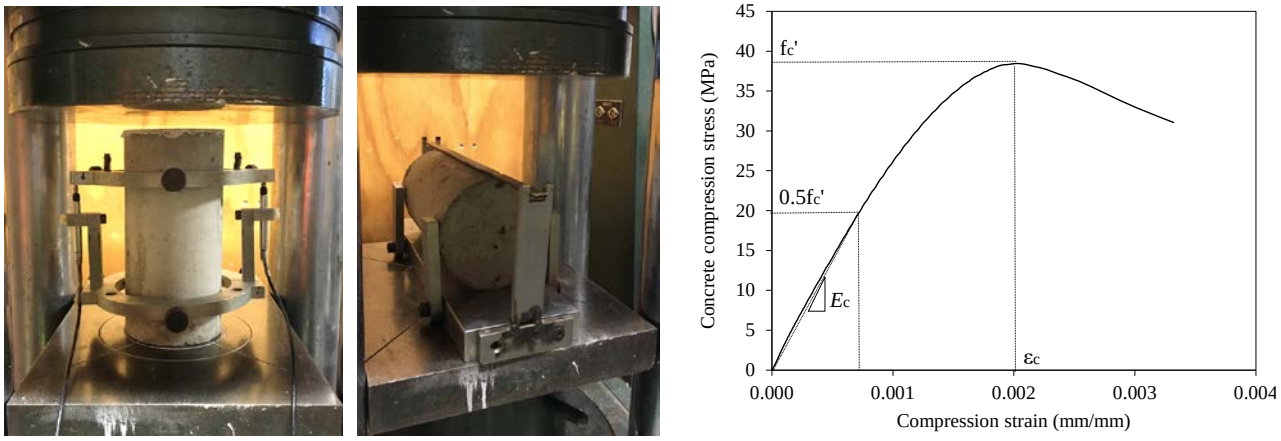

(a) (b) (c)

Figure 7 Concrete cylinder test: (a) compression test setup; (b) split test setup; (c) compression stress-strain curve of Cylinder 1 for wall C1

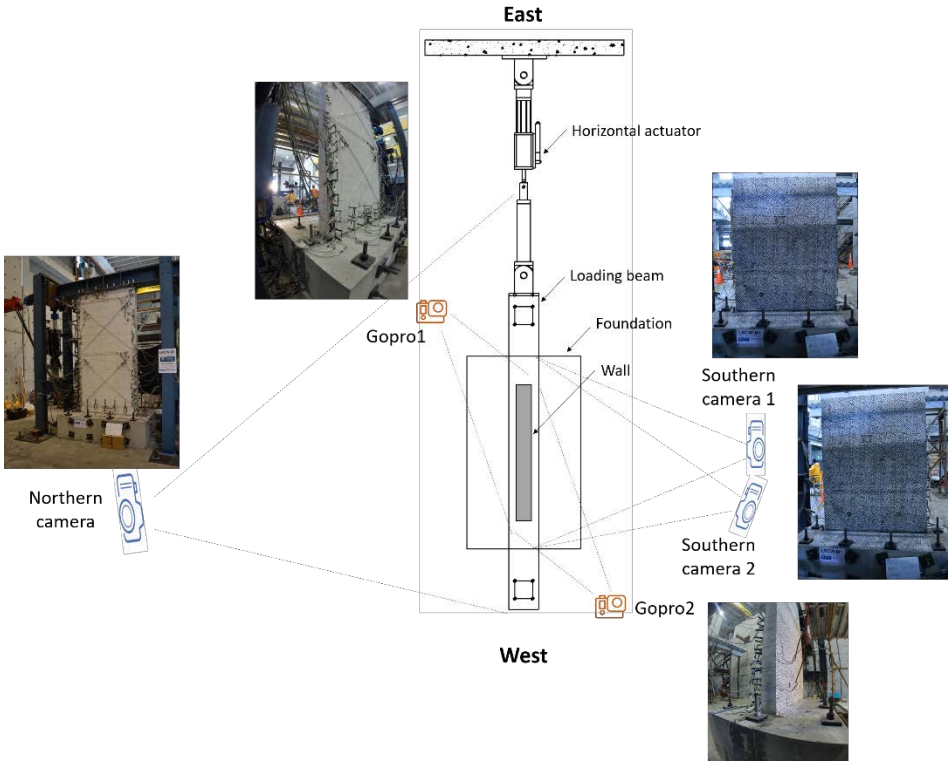

Figure 8 Still camera plan

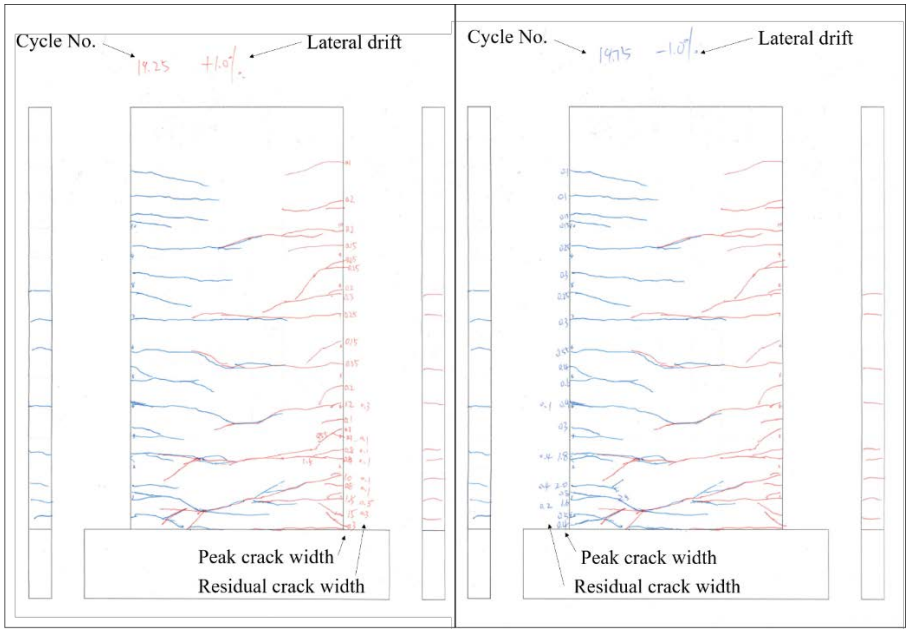

Figure 9 Crack map drawings for wall M4 during first cycle at lateral drift of ±1.0%

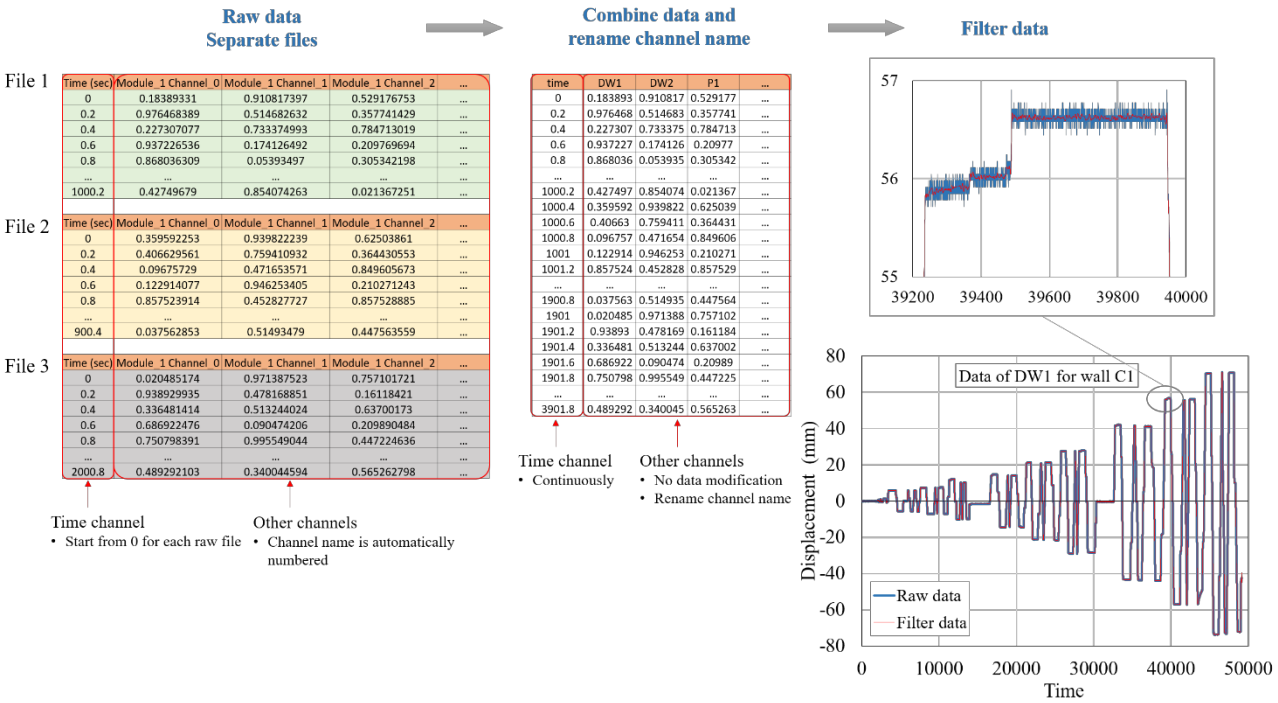

Figure 10 Data processing illustration

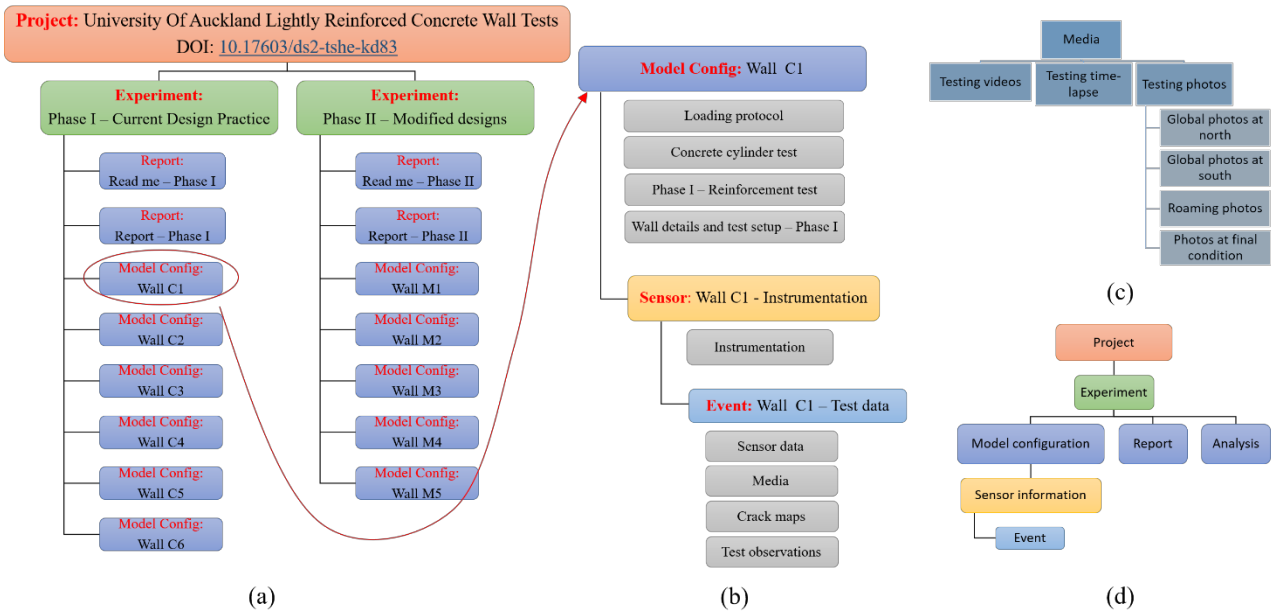

Figure 11 Dataset organization: (a) main structure; (b) data structure in each wall folder; (c) structure in Media; (d) structure in DesignSafe-CI

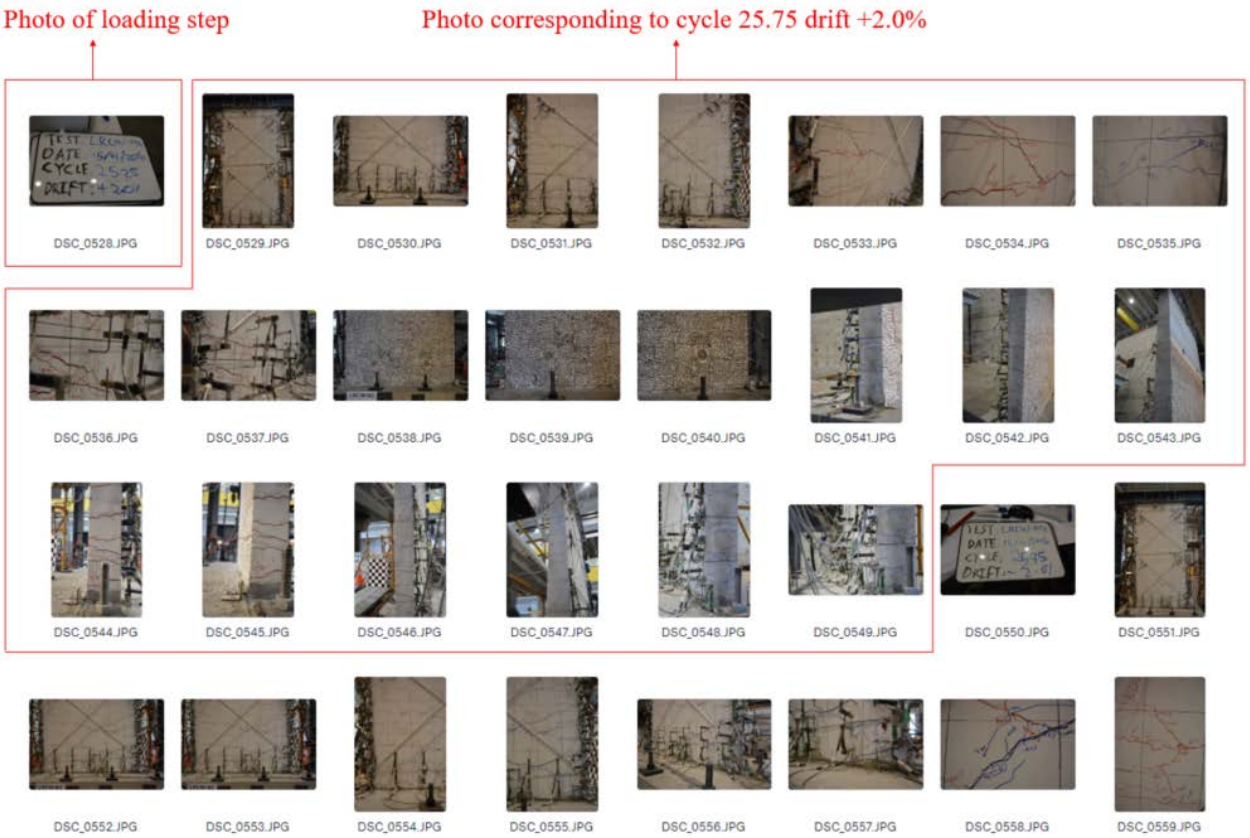

1

2 Figure 12: Example of roaming photo step identification

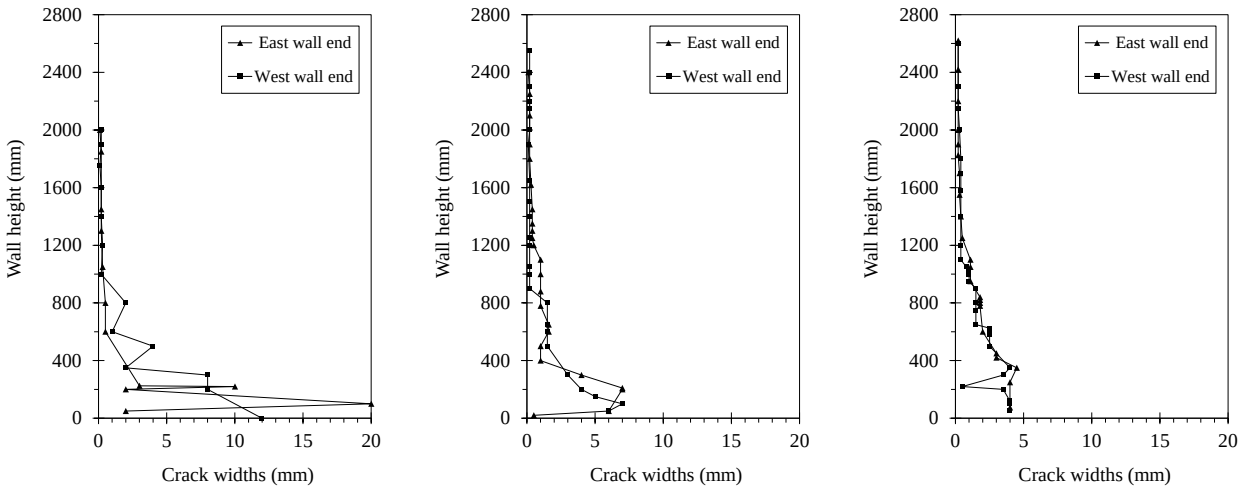

(a) (b) (c)

3 Figure 13 Crack widths at 2.5% lateral drift for test walls: (a) C6; (b) M1; (c) M2

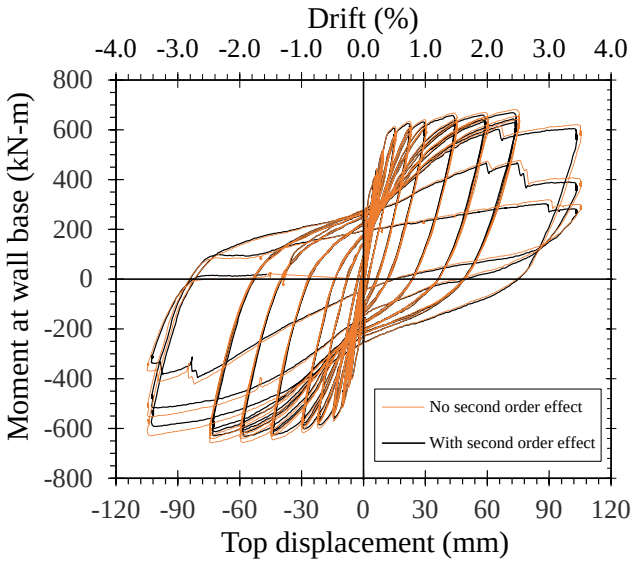

1

2 Figure 14: Comparison of the hysteric curves with and without considering second order effects

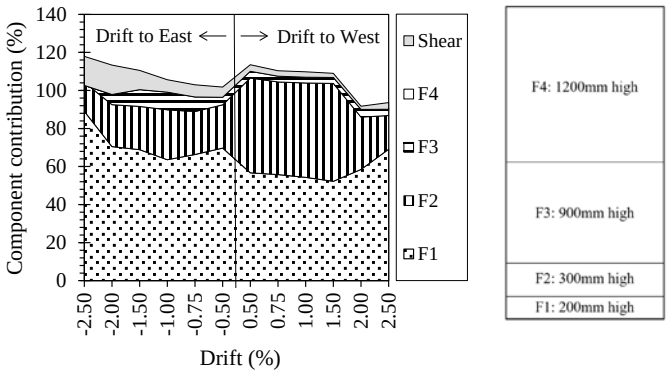

3 Figure 15 Displacement components of wall C1

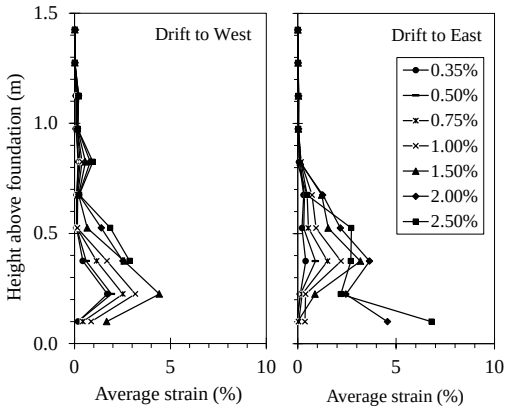

4

5 Figure 16 Average strains along the corner bars of wall C1

6

References

ACI 318-19. (American Concrete Institute) (2019)."Building Code Requirements for Structural Concrete (ACI 318-19) and Commentary." *ACI 318-19*, Farmington Hills, Michigan, American Concrete Institute.

ACI 374.2R-13. (American Concrete Institute) (2013)."Guide for Testing Reinforced Concrete Structural Element under Slowly Applied Simulated Seismic Loads." *ACI 374.2R-13*, Farmington Hills, Michigan, American Concrete Institute.

ACI ITG-5.1-07. (American Concrete Institute) (2008)."Acceptance Criteria for Special Unbonded Post-Tensioned Precast Structural Walls Based on Validation Testing and Commentary." *ACI ITG-5.1-07*, Farmington Hills, Michigan, American Concrete Institute.

AS/NZS 4671. (Standards Australia/Standards New Zealand) (2001)."Steel reinforcing materials." *AS/NZS 4671*, Sydney, Wellington, Standards Australia/Standards New Zealand.

Kam, W. Y., Pampanin, S. and Elwood, K. (2011). "Seismic performance of reinforced concrete buildings in the 22 February Christchurch (Lyttelton) earthquake." *Bulletin of the New Zealand Society for Earthquake Engineering*, 44(4): 239-278.

Lu, Y. (2017). "Seismic design of lightly reinforced concrete walls." PhD thesis, University of Auckland, Auckland, New Zealand.

Lu, Y., Gultom, R. J., Ma, Q. Q. and Henry, R. S. (2018). "Experimental validation of minimum vertical reinforcement requirements for ductile concrete Walls." *ACI Structural Journal*, 115(4): 1115-1130.

Lu, Y. and Henry, R. S. (2017). "Numerical modelling of reinforced concrete walls with minimum vertical reinforcement." *Engineering Structures*, 143: 330-345.

Lu, Y. and Henry, R. S. (2019). "University of Auckland Lightly Reinforced Concrete Wall Tests." https://doi.org/10.17603/ds2-tshe-kd83. DesignSafe-CI.

Lu, Y., Henry, R. S., Gultom, R. and Ma, Q. T. (2017). "Cyclic Testing of Reinforced Concrete Walls with Distributed Minimum Vertical Reinforcement." *Journal of Structural Engineering (United States)*, 143(5).

NZS 3101:2006. (Standards New Zealand) (2006)."Concrete Structures Standard (Amendment 2)." *NZS 3101:2006*, Wellington, New Zealand, Standards New Zealand.

NZS 3101:2006. (Standards New Zealand) (2017)."Concrete Structures Standard (Amendment 3)." *NZS 3101:2006*, Wellington, New Zealand, Standards New Zealand.

NZS 3112.2:1986. (Standards New Zealand) (1986)."Methods of Test for Concrete Part 2: Tests Relating to the Determination of Strength of Concrete." *NZS 3112.2:1986*, Wellington, New Zealand, Standards New Zealand.

Rathje, E. M., Dawson, C., Padgett, J. E., Pinelli, J. P., Stanzione, D., Adair, A., Arduino, P., Brandenberg, S. J., Cockerill, T., Dey, C., Esteva, M., Haan, F. L., Hanlon, M., Kareem, A., Lowes, L., Mock, S. and Mosqueda, G. (2017). "DesignSafe: New Cyberinfrastructure for Natural Hazards Engineering." *Natural Hazards Review*, 18(3).

Sritharan, S., Beyer, K., Henry, R. S., Chai, Y. H., Kowalsky, M. and Bull, D. (2014). "Understanding poor seismic performance of concrete walls and design implications." *Earthquake Spectra*, 30(1): 307-334.

1